京都大学防災研究所年報 第 59 号 B 平成 28 年 6 月
Annuals of Disas. Prev. Res. Inst., Kyoto Univ., No. 59 B, 2016

Study on Landslides in Weathered Granite Areas of Hai Van Mountain, Vietnam

Pham Van TIEN, Kaoru TAKARA and Kyoji SASSA(1)

(1) International Consortium on Landslides

Synopsis

ABSTRACT: Located in the Central Region of Vietnam, Hai Van Mountain is one of the highest risk areas prone to landslides that threaten frequently to safe traffic operations of the national transport systems. This area suffered to several serious damages caused by slope failures to infrastructures and environment in the past. This study presents some results obtained by site observations and the use of ring shear apparatus to investigate the failure mechanism of slopes in weathered granite areas of Hai Van Mountain. The most common types of the landslide in Hai Van Mountain including earth slides, rock falls, and debris flows were found through site investigations. Among them, sliding types are characterized by a complex form of rotational and/or translational modes. Shallow landslides were frequently induced by rainfalls due to loose and unconsolidated materials of slopes. Specifically, the physically landslide mechanism was examined on with two different weathered granite samples taken in the study area by using un-drained ring shear apparatus. The laboratory experiments revealed that only less/moderate weathered granitic soil samples (HV2 sample) were susceptible to a high mobility and experienced liquefaction behavior at sliding surface. In contrast, strongly weathered granite samples (HV1 sample) did not show those features under undrained shear stress loading conditions. The results implied that landslides of weakly weathered granite materials are highly susceptible to rapid motion while the strongly weathered granite materials is not apt to move at the high speed. Another key point, less weathered granite materials are more vulnerable to rainfall-induced landslides because its shear resistance strength was weaker than that of heavy weathered granites under the rainfall impact (Tien et al., 2015). This significant finding was agreed with the evidence and the results from site observations.

Keywords: Hai Van, landslides, granite, mechanism, ring shear apparatus, sliding surface liquefaction

1. Introduction

The study area is Hai Van Mountain that is located in the north of Da Nang City, central region of Vietnam with the geographical position at 16°11′ N of north latitude and 108°7′ E of east longitude in a transition zone of the northern and southern climate. The mountain belongs to Annamite Mountain Range in Indochina Peninsula and stretches to the sea with height ranging from 500 m to 1,500 m above sea level. The range divides the Mekong drainage on the west from the South China Sea drainage on the east. Hai Van Mountain is crossed by two main transport lifelines, including the north-south highway and railway (Fig. 1).

The mountain is widely known as one of the most landslide risk hotpots in Vietnam. Slope failures frequently took place in this area, which seriously destroyed transportation infrastructures and threatened operation safety along 21 km of the

national railway and near 30 km of the national highway in Hai Van Mountain. Notably, the area was confronted by the hardest hit of the 1999 historic storm that triggered numerous sliding, earth flows and debris flows along the transport systems with about 2 million m³ in total volume (Tam, 2005). Landslides induced by rainfalls derived from the storm initiated from 3rd November in a large area of Hai Van Mountain.

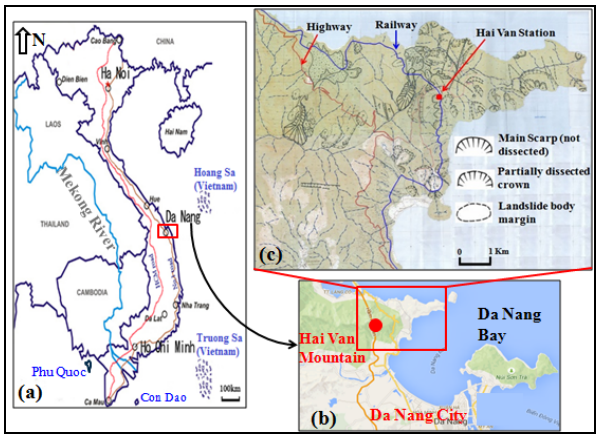

Fig. 1 (a) Location of Da Nang City; (b) Hai Van Mountain and (c) Study area modified from landslide classification map created by Miyagi, 2015

The occurrence time of slope failures and rainfalls derived from the 1999 storm at Da Nang Meteorological Observatory 20 km far from Hai Van Mountain is presented in Fig. 2.

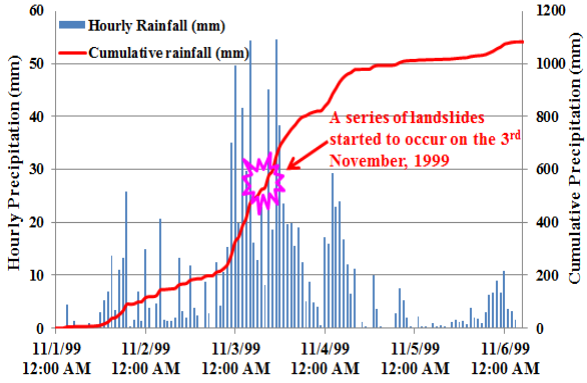

Fig. 2 Cumulative precipitation at the Da Nang gauge station for the period from Nov 1 to Nov 6, 1999 and landslide occurrence in time.

As can be seen, the accumulative precipitation was recorded to 1,074 mm during 6 days of which the rainfall of 512 mm was produced on 3rd November only. While the cumulative precipitation of 1,851 mm during the storm period was monitored at Nam Dong Rain-gauge Station which is about 35 km from Hai Van Mountain. In such disasters, landslide phenomena occurred between more than 20 segments of the national highway separately, which caused interrupted the operation of the road for 8 days and seriously destroyed infrastructures both railway and highway. In addition, according to statistical data of Management Unit for Roads, many slope failures were induced by maximum daily rainfall of 301 mm in November 11, 2007.

2. Regional Settings

2.1 Climatic condition

Hai Van Mountain is located in the region that dominated by severe tropical monsoon climate with the annual precipitation mostly ranging from as much as 2,000 mm to 3,500 mm. The rain and storm season lasts 4 months, from September to December, but it provides with about 70-80 % of the total precipitation.

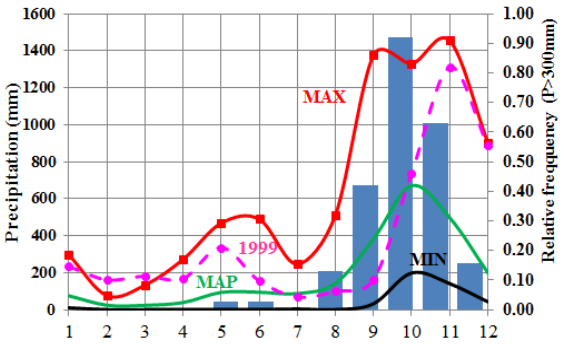

Fig. 3 Monthly distribution of rainfall at Da Nang Meteorological Observatory in the 1976-2013 periods

The mean annual precipitation (MAP), minimum annual precipitation (MIN) and maximum annual precipitation (MAX) are shown for the period from 1976 to 2013 recorded at Da Nang rain gauge station (Fig. 3). As illustrated in the Fig. 3, the available historical record indicates that monthly rainfalls exceeded 300 mm are as much as 75 times (of 114 in a total) in the period from October to December for the 38 years with a maximum monthly value of 1,453 mm in November 2011. The dashed and broken violet line shows monthly precipitation for 1999 (the left axis). The bars show relative frequency of monthly events when rainfall exceeds 300 mm (the right axis). About 92% of monthly rainfalls are larger than 300 mm in October. A relative frequency is calculated by dividing number of events exceeding 300 mm/month by the observed period.

2.2 Geological condition

Hai Van Mountain is characterized by the granitoid Hai Van massif at Triassic age with dominantly mineralogical compositions of biotite granite and two-mica granite (Bao et al., 1994) (Fig. 4). The petro-graphical components are composed K-feldspar, plagioclase, quartz, biotite and muscovite while chemical components of rocks are about SiO2 (69,34÷73,92%), Na2O+K2O (6,11÷8,11%) and K2O/Na2O (>1) (Phuc, 2009). A large proportion of K-feldspar mineral dominated in biotite granite whereas two-mica granite is rich in plagioclase which is weathered much faster than feldspar and changed into clay minerals such as kaolinite.

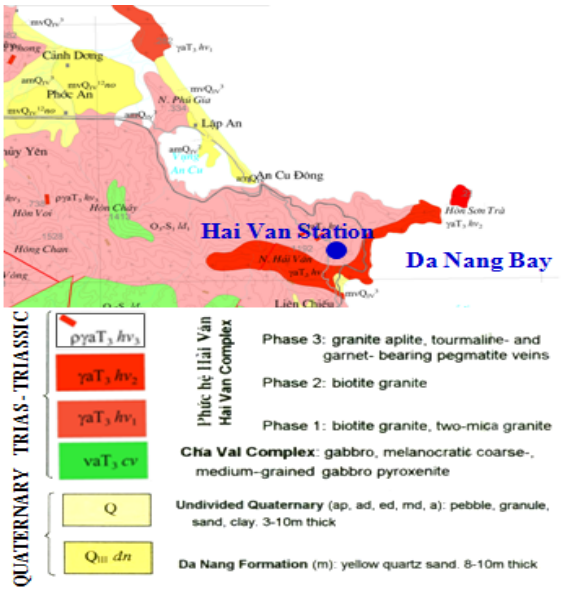

Fig. 4 Geological structure of Hai Van Mountain (Geological Survey of Vietnam, 1995)

3. Methodology

3.1 Site survey and soil sampling

To explore the characteristics of slope failure and examine contributing factors to its occurrences in Hai Van Mountain, the author conducted site observations in detail in May 2014 and December 2015. In these trips, granitic soil samples of slope failures were collected to study its physical mechanism based on ring shear tests in the lab.

3.2 Ring shear tests

The un-drained portable ring shear apparatus (ICL-1), which is able to keep un-drained condition up to 1 MPa of normal stress and pore-water pressure was employed in this study. The ring shear apparatus has a high capability to reproduce the formation and motion of landslides under different stresses due to gravity, seismic force or pore-water pressure on soil specimen taken in the field. Because this device allows shearing at unlimited deformation of the soil samples and monitoring what happens during shearing such as formation of sliding surface, generation of excess pore-water pressure, possible sliding surface liquefaction, failure and post-failure deformation characteristic at large displacement because it allows (Sassa et al., 2014).

The apparatus has three main components separately, including: (1) Instrument box, (2) Monitoring box and (3) Control box (as shown in Figure 6 from left to right).

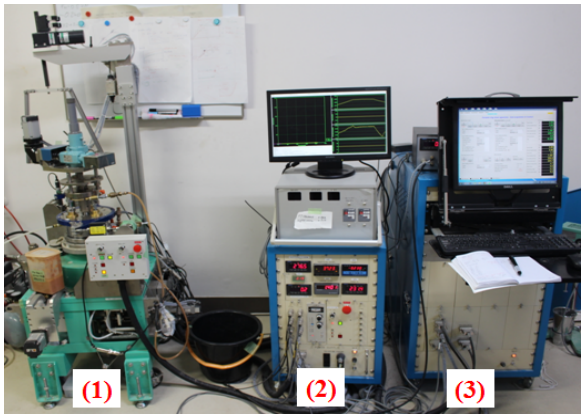

Fig. 6 Portable Ring Shear Apparatus (ICL-1)

An updated version of ring shear apparatus ICL-1 with structural modifies is illustrated in Fig. 7. In which, the structural design of normal stress loading system and rubber edge has some changes compared with the original one (the version designed to donate to SATREPS project in Croatia). Firstly, normal stress loading system was upgraded by electric servo motor instead of using an oil pressure piston loading system to generate the normal stress. Secondly, rubber edge in the gap to keep un-drained condition was also changed with a new design. The difference appears on the placement of rubber edge at the lower shear box and a Teflon Ring horizontally supporting the rubber edge.

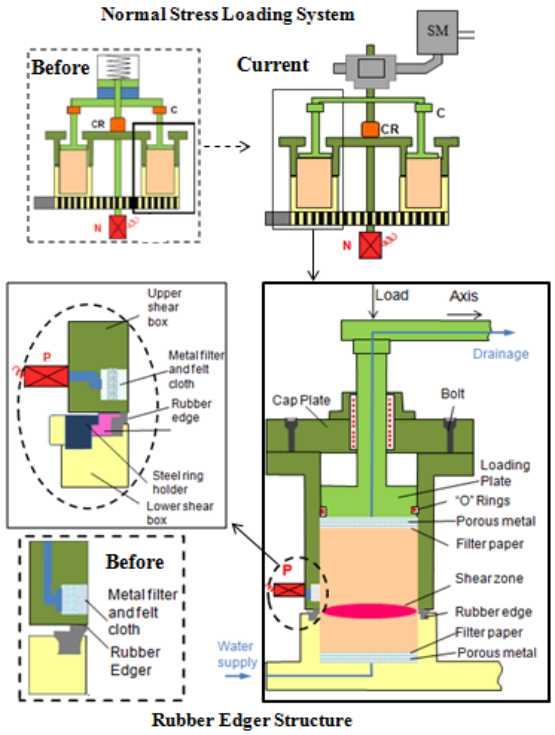

Fig. 7 Structural changes of the latest ICL-1 version: The differences in normal-stress loading system and rubber edge structure before and after 2014

3.3 Testing procedures

Firstly, the landslide prone samples were prepared to be fully saturated with de-aired water in a vacuum tank. Next, the gap adjustment was conducted by giving an initial contact pressure from 0.8 kN to 1 kN between the upper pair of rings and the rubber edges using the gap control. The gap value was kept constant during tests to maintain un-drain conditions and to prevent leakage of water and sample under high-speed shearing.

After installing the shear box, the CO2 and de-aired water circulations were executed to let all bubbles of air come out from the shear box. Then, water leakage and rubber edge friction tests were also made for checking un-drained condition of all tests before building saturated samples inside the shear box. The degree of saturation was checked indirectly by calculating the ratio (BD) of excess pore-pressure increment and normal- stress increment under un-drained condition. The term of BD ratio was proposed by Sassa (1988). In this study, un-drained tests were usually carried out with BD $\geq$ 0.95.

Landslide prone samples of the sliding surface were consolidated before shearing. The initial shear stress and normal stress due to the weight of the soil mass above the sliding surface were applied slowly to reproduce an initial stress state same as field conditions. Finally, ring shear simulations of landslides were carried out by applying different modes of shearing in corresponding to practical conditions triggering landslide phenomena such as shear speed control tests and cyclic loading control test. In this study, since a depth of the potential sliding plane of landslides was estimated in site investigation ranging from 10 m to 20 m, the parameters of 230 kPa for normal stress and 120 kPa for shear stress were used in the calculation of the initial stress corresponding to 15 m in depth and a slope angle of 26 degrees.

4. Results

4.1 Site investigation results

The site investigations showed that shallow landslides occurred on the slopes of less weathered granite are dominant in the study area. The location and the description of landslides visited in 2014 were presented in Table. 1.

Slope failures and landslides are mostly concentrated along national transport system (including the highway and railway lines) and contiguous zone to South China Sea. The extent, location and types of slope failures can be found in a landslide classification map created by Prof. Miyagi in 2015 as an output of the SATREPS project in Vietnam (see in Fig. 1 above).

(1) Weathering of granite and slope failures

From a lithological point of view, the area is considered to be homogeneous as most of it is covered by various materials of weathered granitic rocks with diversified degrees of weathering process. Qualitatively, geological structure of slopes consists of three material layers on slope at least, namely loose sediments (alluvium/colluviums), strong and less weathered granitic rocks and bedrock of granite mass. The mass of weathered granitic rocks is covered by a thin sedimentary layer of 1 m to 3 m in depth and several single boulders. The granite masses with many cracks and joints in different direction were observed visually. Those features were found in the site survey clearly. Granitic rocks are fresh or very completely strong or less weathering or

partly weathering in different layers and different directions (Fig. 8). Thus, formed materials are very different from grain size distribution, mineral composition, colors and hardness grade. As for a completely weathering degree, granitic rocks were changed into soil-like materials with brown, yellow and white colors and are very soft and slightly soft. Other partly weathering degree, material of granitic rocks is a mix of soil and stones with different grain sizes. Such kind of materials is a bit hard with red and grey colors mixing with a speckled mineralogical composition in black color. The more weathering materials are softer and finer than others. Materials of weathered granitic rocks are very loose and unconsolidated. They are very easily to be eroded by rainwater and become earth flows.

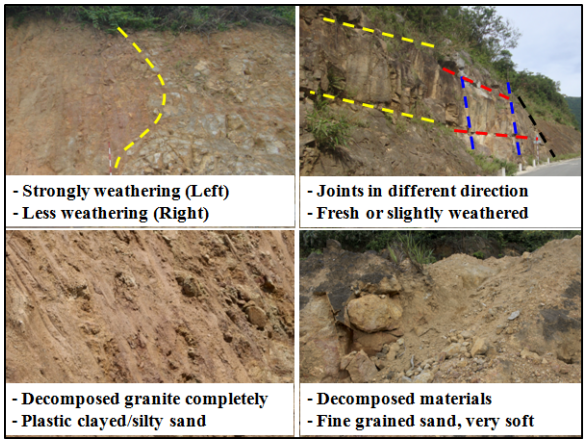

Fig. 8 Weathered granitic materials on slopes

Table 1 Location of landslides and its description

No.	Location		Description/ Landslide types	Degree of the weathering	State	Estimated dimensions			
	Longitude	Latitude				Width (m)	Length (m)	Depth (m)	Slope angle (degree)
1	108° 8'6.22"E	16°11'44.14"N	Debris flow	Less	Stopped	30	60	1 - 2	17
2	108° 7'56.24"E	16°12'32.90"N	Debris flow/Earth slides	Less	Stopped	20	50	1	20
3	108° 8'31.21"E	16°12'3.62"N	Landslide/Slump Type	Less/ Moderate	Stopped	35	50	4 - 5	32
4	108° 8'45.42"E	16°12'1.22"N	Rockfalls	Fractured rocks	-	-	-	-	-
5	108° 8'46.31"E	16°11'58.63"N	Shallow landslide/Fall type	Less	Stopped	20	30	2	31
6	108° 8'46.86"E	16°11'56.90"N	Rockfalls	Less/ Moderate	-	-	-	-	-
7	108° 9'11.04"E	16°12'0.81"N	Rockfalls	Fractured rocks	-	-	-	-	-
8	108° 8'58.22"E	16°11'58.67"N	Shallow landslide/Slump type	Less	Stopped	10	15	4 - 5	20
9	108° 9'5.68"E	16°11'45.78"N	Large-scale landslide/Transitional Slide	Less	Active	100	210	10 - 13	25
10	108° 8'40.68"E	16°11'26.70"N	Shallow slope failure	Less	Stopped	150	300	5 - 10	25
11	108° 9'3.80"E	16°11'37.56"N	Hai Van station large-scale landslides/Transitional and Rotational Slide	Very different	Active	200	400-600	15 - 20	26
12	108° 9'3.80"E	16°11'37.56"N	Hai Van station large-scale and deep-seated landlides/ Transitional type	Very different	Active	450-500	600-800	35 - 45	22

In Hai Van Mountain, warm and wet conditions of the tropical climate strongly influence slope materials involved in landslides, because the rapid weathering processes under humid conditions strongly weaken and deteriorate its regolith covers. The degrees of weathering of granitic rocks in Hai Van area are very different and show a large diversity in depth, texture, landform, chemical-mineral components, geological characteristics and origin. Slope materials are mainly products of weathered granites in poorly or unconsolidated materials.

(2) Characteristics of slope failures

The most common types of landslide in Hai Van Mountain are earth slides, rock falls and debris flows. In which, sliding types are characterized by a complex form of rotational and/or translational modes (Fig. 8).

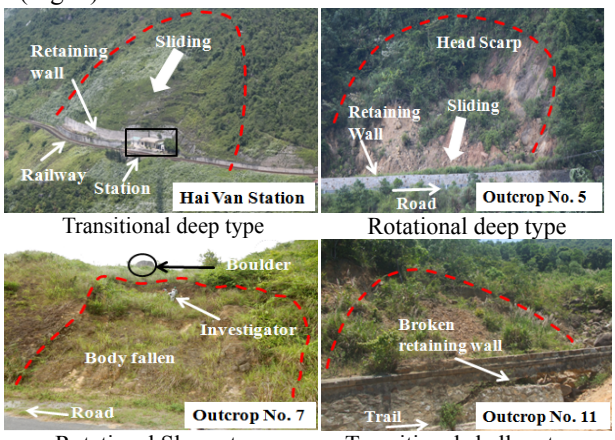

Fig. 9 Type and description of investigated landslides

The movement of landslide material may vary from abrupt collapses (the outcrop No. 5) to slow gradual slides (landslides on the slope behind the Hai Van station). Landslides are at different scales in both shallow and deep types, which depend on the thick of residual soil on slopes, weathering degrees of granitic rocks and fracture zones. The shallow landslides have a volume of 50 m³ to 500m³ with a depth of sliding surface about 2 m to 5 m. Shallow landslides were frequently induced by rainfalls due to a loose and unconsolidated material of slopes. More specifically, landslides are mainly populated a long national highway while large-scale and deep-seated landslides are situated next to the railway or at the edge of steep mountains. In the region, at least five deep- seated landslides were found around Hai Van Station, which have a volume ranging from several hundred thousand 200,000 m³ to several million m³. The estimated depth of potential sliding surfaces of those large-scale landslides in Hai Van Mountain often ranges largely about 5 m up to 50 m. Besides, site investigation revealed that most of failures were found with regards to artificially modified slopes (cutting/filling slopes for road constructions) and only several slides occurred on natural slopes.

Since slope materials are formed from weathered granite, landslide occurrences directly relate to its weathering manner and grade. In this regard, a majority number of landslides were found in the less weathered granite areas than its occurrence in the slopes of heavily weathered granitic rocks. The reason is because of a very quiet difference between two kinds of granites of which the connectivity of strongly weathered materials is much firm while less weathered materials are isolated and easy to loosen and erode. Clearly, kaolinite mineral in heavily weathered materials is well connected to bind soil grains.

4.2 Soil Properties

Two suspected landslide samples, namely a less weathered granitic rocks sample and a strong weathered granitic rocks sample (hereinafter called as HV2 sample and HV1 sample, respectively), were taken to study on their shear behavior during motion and post-failure by ring shear simulator (Fig. 5).

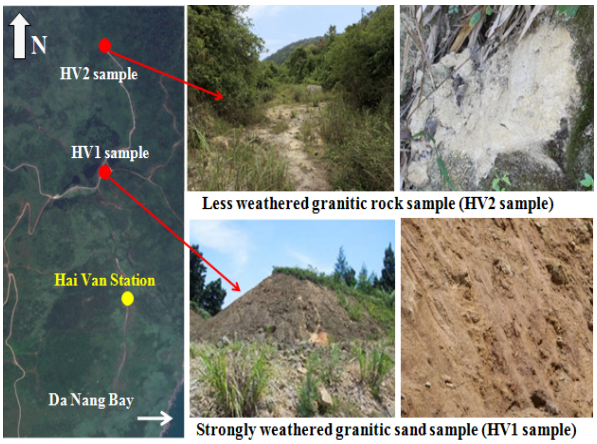

Fig. 5 The locations of soil sampling

Landslide prone samples were tested in the laboratory to obtain basic parameters by standard laboratory tests including physical soil properties (Table 2) and grain-size distribution (Fig. 10).

Table 2 Properties of soil samples

Parameters	Value	
	Haivan-1 sample	Haivan-2 sample
Specific gravity, Gs	2.67	2.64
Wet unit weight, γt	20.15	17.65
Dry unit weight, γd	16.32	12.82
Void ratio (e)	0.64	1.05
Permeable coefficient, k (cm/sec)	5x10E-5	3x10E-4

The grain size distribution curves showed that HV1 sample contains clay-like fine grains much more than HV2 sample. Basically, HV1 sample is slightly clayed sand, while HV2 sample is sand. Both materials are fine to coarse grained with fine gravels and mica fragments.

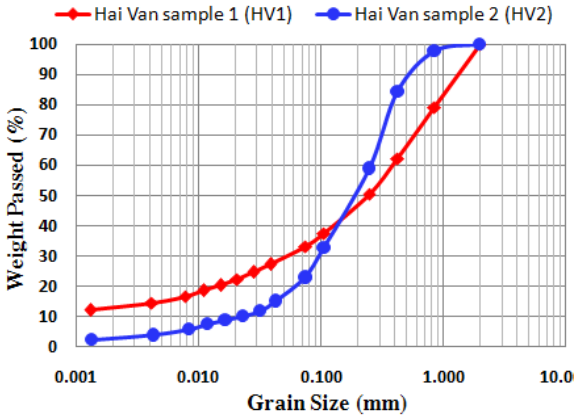

Fig. 10 Grain-size distributions of two samples

4.3 Ring shear results

(1) Undrained shear stress control tests

Undrained monotonic shearing was carried out to explore landslide mechanism and to observe the pore water pressure generation as well as initiation of failure motion. Test results showed that excess pore water pressure generated during shear displacement after failure of HV2 sample, but there was not much pore water pressure increasing during shearing (Fig. 11 & 12). Seen from results, the steady state shear resistance of HV1 sample was 93.2 kPa while HV2 sample obtained 5.9 degrees of apparent friction angle. The peak friction angle of HV1 sample and HV2 sample are around 41.0 degrees and 36.0 degrees with 143.5 kPa and 133.1 kPa maximum shear resistance, respectively. Friction angle during motion of two landslide samples at large displacement are about 38.0 degrees for clayed/slightly clayey soil and 33.5 degrees for sand.

(2) Rainfall-induced landslide simulation

Rainfall-induced landslides were produced by increasing gradually pore water pressure simulating a rise of groundwater level during rainfalls. In these tests, both samples were consolidated to 230 kPa in normal stress and 120 kPa in shear stress. Pore water pressure was then increased up to 200 kPa at the rate of 1.5 kPa/sec for HV2 sample and at the lower rate of 0.2 kPa/sec for HV1 sample due to its low permeability.

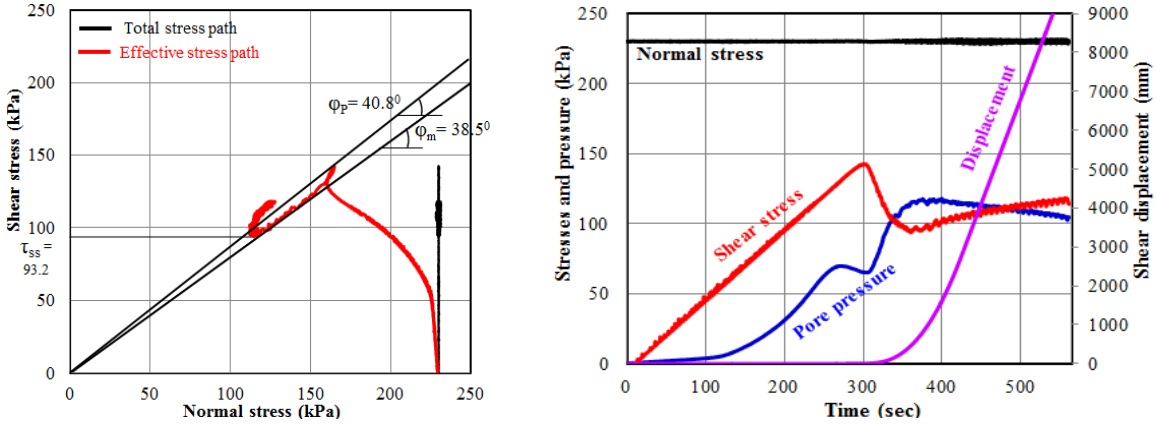

Fig. 11 Effective stress path (left) and time series (right) of shear stress control test for HV1 sample

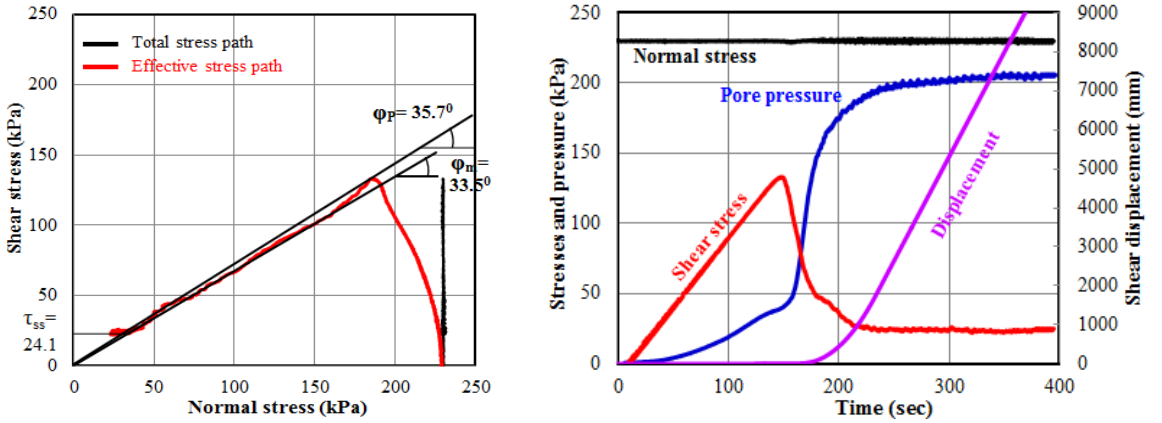

Fig. 12 Effective stress path (left) and time series (right) of shear stress control test for HV2 sample

The test results of two landslide samples are shown in the Fig. 13 and Fig. 14, with a red color line showing effective stress path and a black color line showing total stress path. The results indicate that HV1 sample failed around 95 kPa of pore water pressure increment while failure occurrence of HV2 sample was earlier to occur with about 80 kPa of additional pore water pressure value. The critical pore pressure ratios of HV1 sample and HV2 sample (r_{u1} and r_{u2}) are 0.41 and 0.34, respectively, in which the parameter of r_u is defined as a ratio of pore water pressure increment triggering failures and its normal stress). For the HV1 sample, the friction angle at peak (φ_P) stayed at about 41.3 degrees and for the HV2 sample, this angle value was only 36.4 degrees.

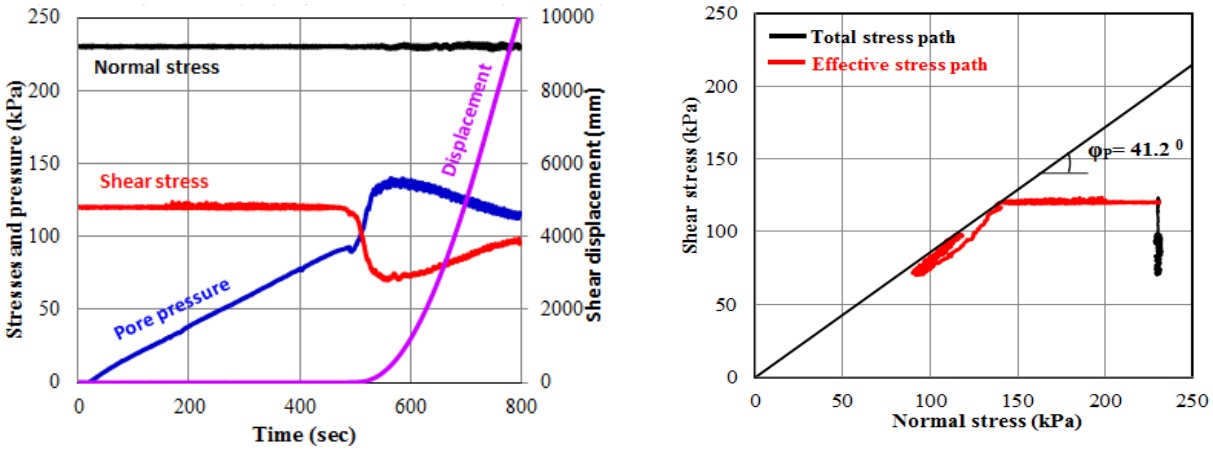

Fig. 13 Time series data and effective stress path of pore-water pressure control tests on HV1 sample

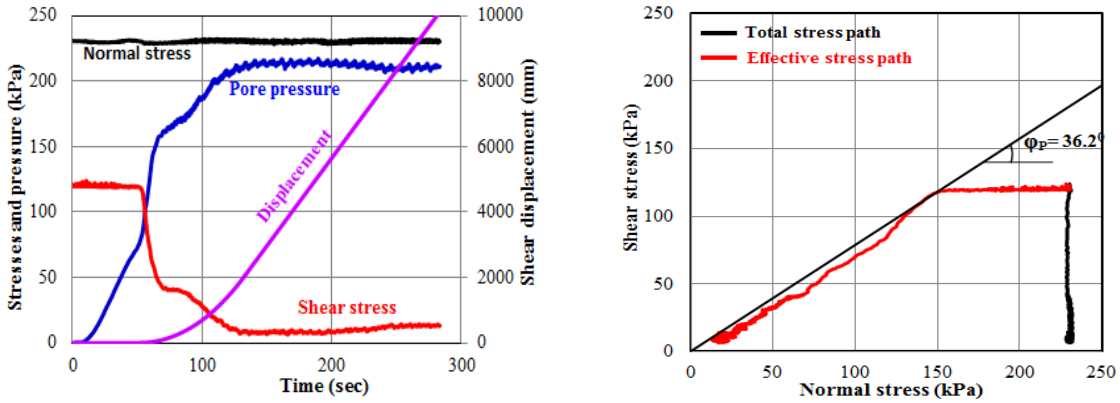

Fig. 14 Time series data and effective stress path of pore-water pressure control tests on HV2 sample

5. Discussions

Failure characteristics of two landslide prone samples are greatly different in undrained ring shear tests. Basically, HV2 samples at sliding surface were completely liquefied during shearing at large displacement because of excess pore-water pressure generation whereas the failure of HV1 sample did not seem to experience the sliding surface liquefaction due to very less value of pore water pressure. For this reason, landslides of HV1 sample could not move at a high velocity while landslides of HV2 sample are characterized by a rapid movement during shearing. The difference of Hai Van landslide mechanism mainly depends on such liquefaction behaviors in both samples, which results from differences in the nature of the weathered material under undrained condition. In this regards, HV1 sample shows behavior of clayed soils or silty sand like a dilative behavior while shear behavior of HV2 sample is very similar to coarse sands showing a contractive behavior. Therefore, HV1 sample is not prone to liquefaction behavior at sliding surface because its material is not susceptible to be crushed during shearing tests. In contrast, HV2 sand sample is more susceptible to grain crushing and sliding liquefaction. Consequently, the mechanism of rapid motion of the landslides only occurs in the tests of HV2 sample while HV1 sample would not show a mobility behavior.The term of sliding surface liquefaction (Sassa, 1996 and 2000) mentions to the behavior of shearing zone due to grain crushing of samples. Grains in the shear zone are crushed during shearing and the soil structure was subjected to volume reduction. A grain crushing leads to excess pore water pressure generation and a rapidly consequent reduction in effective stress resistance strength. The mechanism of sliding surface liquefaction is explained comprehensively in Fig. 15.

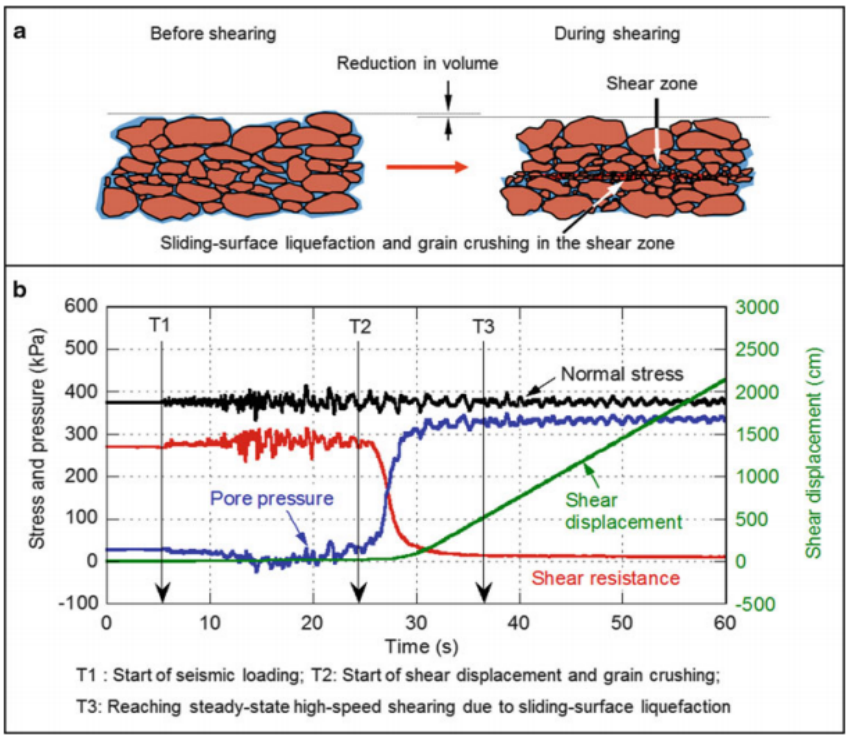

Fig. 15 Explanation of the mechanism of sliding surface liquefaction

As seen in Fig. 15 above, T1 in Figure 2B is the onset of seismic loading. Under the loading condition pore-water pressure started to decrease immediately. It is explained that dilatancy occurred which is a characteristic of dense materials. T2 in Figure 2B shows a starting point of post-failure shear displacement. Value of pore pressure accelerates progressively to close to normal stress and remain unchanged. The normal stress at steady state (σ_{ss}) is mainly the difference between normal stress and pore water pressure correspondingly. T3 in Figure 2B is the start of steady state high speed motion like rapid landslide motion. The mobilized shear resistance at this stage is mainly steady state shear resistance. The ring shear simulation will reproduce a rapid motion of landslides.

To examine how grain crushing of samples occurred at sliding surfaces, after the shear test was finished, both disturbed and undisturbed samples were collected from the shear zone and other than sliding zone of the shear box; then grain-size analysis was performed on these samples (Fig. 16). Grain-crushing, sliding plane and liquefied materials of two difference landslide tests are compared and denoted in Fig. 17 below.

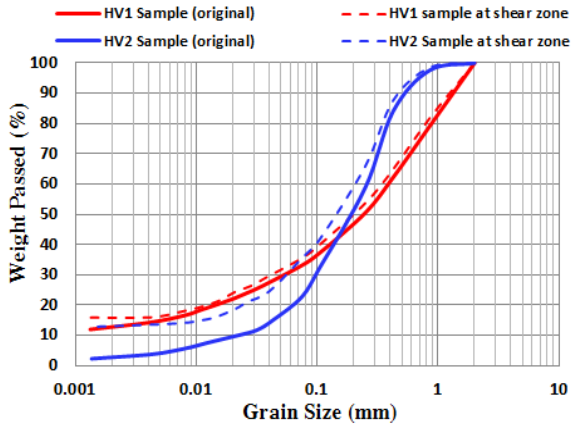

Fig. 16 Grain-size distribution of two samples at the sliding surface after shearing until 10m in compared with two original samples

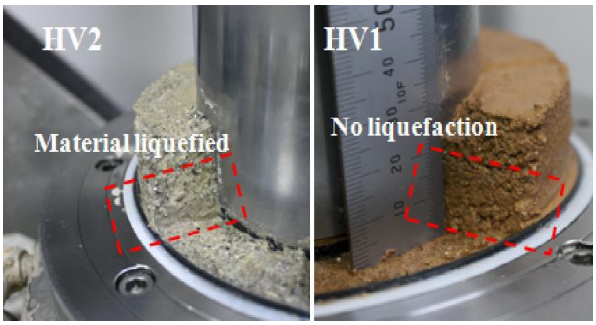

Fig. 17 Photograph of the sample HV2 and HV1 after failure

6. Conclusions

Hai Van landslides were induced by combination of contributing factors including climatic, morphological and geological conditions of weathered granitic area as well as triggering factors like extreme rainfalls. In the weathered granitic rock area of Hai Van Mountain, slope failures can be categorized as rotational-transitional form or slump type. Among them shallow landslides are dominant in the whole study area. Besides, another type of landslides is debris flow which occurs on the surface layer of weathering granitic rock materials or a sedimentary layer.

The mechanism of the Hai Van station landslides can be interpreted through a series of ring shear tests conducted on the samples of suspected sliding plane. The motion of those landslides could be dominated by mobility behavior of the clayed layer (HV1 sample) and the sand layer (HV2 sample). As analyzed above, the difference in un-drained shear behaviors of two samples HV1 and HV2 resulted in the difference of landslide characteristics in Hai Van Mountain. In regard of this, mechanism of rapid motion of the landslides only occurs in the HV2 sample (less weathered granitic soil samples). In contrast, HV1 sample (strong weathered granitic soil samples) has not shown a mobility behavior. Meanwhile, monitored results showed that landslides are more likely to occur on slopes of less weathering granitic rocks than their occurrences in slopes of strong weathering granitic rocks under the rainfall impact due to lower shear strength parameters of the sample in the less weathering granitic rocks region. The evidence of slope failures dominated in areas of less weathered granite was not only agreed to the findings in site observations but it is similar like findings from previous researches on landslides in weathered granitic rocks regions, which was found by other researches worldwide. The prediction of landslide sites in Hai Van Mountain based on its physical mechanism has an important significance for landslide risk assessment in the future.

References

Bao, N.X, Luong, T.D, Trung, H. (1994): Explanatory note to the geological map of Việt Nam on 1/500,000. Geological survey of Vietnam.

Ostric, M., Liutic, K., Krkac, M., Sassa, K., Bin, H., Takara, K., Yamashiki, Y. (2012): Portable Ring Shear Apparatus and its application on Croatia Landslides, Annuals of Disaster Prevention Research Institute, Kyoto University, No. 55B, pp. 57-65.

Phuc, L.D. (2009): Granitoid Petrology of Hai Van Massif. Science & Technology Development, Vol 12, No.05, pp. 46-54.

Sassa, K., He, B., Dang, K., Nagai, O., Takara, K. (2014): Plenary: Progress in Landslide Dynamics. Landslide Science for a Safer Geo-environment (Sassa, Canuti, Yin eds), Vol.1, pp.37-67.

Sassa, K. (1996): Prediction of earthquake induced landslides. Proceedings of 7th International Symposium on Landslides. A.A. Balkema. Trondheim, 17-21 June, vol 1, pp. 115-132.

Sassa, K. (2000): Mechanism of flows in granular soils.

Proceedings of GeoEng2000, Melbourne, vol 1, pp. 1671-1702.

Tam, D.M., Hanh, N.H, et al. (2008): Research on Selection and Application Conditions of the New Technologies for Landslide Risk Prevention along National Highways. Research project in transportation sector, Ministry of Transport, 2008, 396 pages (in Vietnamese).

Tam, D.M. (2005): Report on the causes of slope failure at Hai Van station and a proposal of countermeasures. Research project in transportation sector, Ministry of Transport, May 2005, 18 pages (in Vietnamese).

Tien P.V., Sassa, K., Takara, K., Khang D., Loi D. (2015): Analyzing Failure Characteristics and Potential of Landslides in Hai Van Mountain, Vietnam. Proceedings of the 10th Asian Regional Conference of IAEG, Kyoto, Japan, pp. 586-591.

Tien P.V., K. Sassa, K. Takara, Binh H.T., Luong L.H. (2015): Characteristics and failure mechanism of landslides in weathered granitic rocks in Hai Van mountain. “Proceedings on International conference on landslides and slope stability 2015”, pp. 165-172.

(Received June 13, 2016)